Networked Energy Cooperation in Dual Powered Green Cellular Networks

Ashutosh Balakrishnan, Swades De, and Li-Chun Wang

***Abstract*—Designing solar-enabled and power grid connected, 'dual-powered', cellular networks is challenging due to the double stochasticity arising from energy harvest and user traffic, resulting in spatio-temporally varying traffic-energy imbalances. Improper strategy to optimize the power grid connectivity results in generation of significant carbon footprint. In this paper, we present an analytical framework to mathematically capture the traffic-energy imbalances in such a dual-powered network and propose to improve the temporal network energy utilization by exploiting these imbalances through a cooperative energy sharing mechanism among the base stations (BSs), via the grid infrastructure itself. The cooperative communication system is designed and optimized independently from two perspectives, namely, grid energy procurement and carbon emission minimization (in carbon free 'energy producer' mode) and operator revenue maximization (in 'energy prosumer' mode). The energy producer mode involves the BSs, without the flexibility to procure energy and acting as distributed energy source to the power grid. The energy prosumer mode provides additional flexibility of grid energy procurement to the BSs in addition to energy sharing and selling. For a given capital expenditure (CAPEX), both the optimization problems are reformulated into convex quadratic problems and closed form expressions for the optimal quanta of energies to be shared/procured through/from the grid are obtained. The optimal CAPEX for the proposed modes of network operation are obtained via linear revenue maximization problem formulation. The results demonstrate that the proposed cooperative energy framework significantly improves the temporal network energy utilization, thereby reducing the grid energy procurement and providing significant revenue gains compared to the state-of-art.**

***Index Terms*—Dual powered base stations, traffic energy imbalance, cooperative energy sharing, green communication, carbon footprint, operator revenue**

I. Introduction

THE Information and Communication Technology (ICT) sector has witnessed rapid strides in the last few decades. The advent of 5G and beyond communications (B5G) powered by the rise of the Internet of Things (IoT) is expected to increase the quality of service (QoS) demands of the networked user equipments (UEs) [2]. Wireless cellular networks are equipped with energy intensive base stations (BSs) in order to cater to the demands of the associated UEs. Conventionally these BSs are powered through non-renewable energy sources (such as, coal, diesel), which generate significant amounts of carbon footprint. For instance, a standalone Marco BS is estimated to consume about 1500 liters of diesel per month [3], [4], which is equivalent to over 4 tonnes of carbon dioxide (CO_2) [5]. The US Energy Information Administration [5] states that the CO_2 emissions resulting from power generation with coal as fuel is 1.002 tonnes per Wh. The surge on user QoS due to B5G communications and IoT is expected to result in a significant increase in BS deployment [6], leading to an increased network energy consumption.

Powering the BSs through purely renewable energy sources (such as, solar, wind, RF) [7]–[10] is an effective solution for reducing the carbon footprint. However, these systems need to be over-provisioned with capital expenditure (CAPEX) as they are prone to be influenced by climate and are not cost effective from the operator's perspective [11]. In recent years, there has been a major thrust on designing scalable networks, to expand telcommunication to the farther rural areas. Accordingly, revenue and cost incurred to the network operator have become essential network parameters in addition to energy efficiency. There is an urgent need for cost optimal and energy efficient solutions, in order to ensure a global rollout of the upcoming B5G communications. To this end, developing renewable energy powered and power grid connected, 'dual-powered' networks [12] have been of interest.

Designing dual-powered systems face double stochasticity arising due to spatio-temporally varying energy harvest and user traffic, leading to *traffic-energy imbalances* across the network. These imbalances result in under-utilization of the temporal network energy and degradation of network performance in terms of user-service and operator revenue [13]. Furthermore, while dual-powered networks reduce operator expenses due to the flexibility of grid energy procurement, they generate significant amounts of carbon footprint. In a recent paper [13], a cooperative coverage adjustment strategy has been proposed to mitigate the effects of traffic-energy imbalances. As a complementary contribution, in this work, we present a cooperative energy sharing framework via the grid infrastructure itself to exploit the imbalances without the flexibility of BS coverage adjustment, to improve the temporal network energy utilization. The system is designed to achieve the significant benefit of cooperative networked

This work was supported in parts by the Science and Engineering Board, DST, under Grant CRG/2019/002293, the INAE under the Abdul Kalam Technology Innovation National Fellowship, the Prime Minister's Doctoral Research Fellowship, the Ministry of Science and Technology under the Grants MOST 110-2221-E-A49-039-MY3, MOST 111-2221-E-A49-071-MY3, and the Center for Open Intelligent Connectivity from The Featured Areas Research Center Program within the framework of the Higher Education Sprout Project by the Ministry of Education (MOE) in Taiwan.

A preliminary version of this work was presented in IEEE GLOBECOM 2021 [1].

A. Balakrishnan is with the IIT Delhi-NYCU Taiwan Joint Doctoral Program and Department of Electrical Engineering, Indian Institute of Technology Delhi, India (email: tiz198343@iitd.ac.in). S. De is with Department of Electrical Engineering and Bharti School of Telecommunication, IIT Delhi, India (email: swadesd@ee.iitd.ac.in). L.-C. Wang is with Department of Electrical and Computer Engineering, National Yang Ming Chiao Tung University, Taiwan, ROC (email: wang@nycu.edu.tw).

operation on grid energy procurement and operator revenue. In the upcoming subsections, we will discuss the related works, contributions, and the organization of the paper.

A. Related works

Traditional strategies to reduce the network power consumption have been optimal resource allocation [14], cell zooming [15], and dynamic BS switching techniques [16]. Recently, the authors of [8] introduced an off-grid purely solar-enabled BS framework for efficient energy allocation to the BSs. In order to improve the profitability of off-grid solar powered systems, dual-powered network frameworks have been presented in [17]–[23].

The authors of [17] have presented a dual battery architecture for profit driven user association, while the framework in [18] has studied an energy model for green networks to provide ancillary services to the grid. The authors of [19] developed an energy efficiency optimization framework in a two-tier network with hybrid powered BSs. The authors of [20] considered a dual-powered framework without the flexibility of inter-BS energy transfer; instead, it proposed to procure energy in case the BS become energy deficient.

Energy sharing among dual-powered BSs has been explored in [21]–[23]. In [21], the authors explored an online energy cooperation framework based on Markov decision process (MDP) to minimize the grid energy acquisition. Energy transfer among the BSs was proposed using a mesh framework of separate power lines between the BSs. The framework presented in [22] improved from the framework in [21] to estimate the optimum mesh connectivity of power lines between individual BSs to facilitate energy exchange between them. Recently, the authors of [23] have also studied energy cooperation among hybrid powered BSs using the Lyapunov optimization framework. The proposed energy sharing framework in [23] is similar to [21], i.e., through a separate mesh network of power lines.

The above studies [21]–[23] did not examine the effect of Spatio-temporal traffic-energy imbalances on grid energy procurement or operator revenues. We believe that it is crucial to investigate and understand the effects of these imbalances in a dual-powered cellular network to manifest useful engineering insights. The frameworks in [21]–[23] have not evaluated closed form expressions for the optimal amounts of grid-energy procurement and the energy transferable to a BS. Additionally, they did not focus on the specific cost aspects of the network, for instance, these frameworks did not discuss the optimal CAPEX required to design their network. We anticipate that using separate power line infrastructure for energy transfer (in addition to the existing power grid infrastructure) will lead to practical challenges like distance dependent power losses [24], and added CAPEX to the operator in laying and maintenance of the power lines. The framework in [22] also considers energy selling among the BSs as well as energy selling between the BSs and the grid.

In contrast, we consider the BSs as a single entity, enabling energy transfer among them via the grid infrastructure itself. It is proposed that the price associated with such an energy transfer be much lower than the prices of energy procurement or selling and is to be borne by the operator for grid maintenance. While the frameworks in [21]–[23] propose to minimize the grid energy consumption, their frameworks still rely on the power grid to ensure seamless operation. We argue that as a carbon-aware alternative, the network can be designed and operated in a carbon free 'energy producer' mode wherein the BSs act as distributed energy producers to the power grid and may not need to procure grid energy, thus leading to self-sustainable green networks.

In [1], we explored the effect of traffic-energy imbalances on operator revenue and grid consumption in a two-BS scenario. In this paper, we extend the idea to a multi-BS dual-powered scenario and present the following contributions.

B. Contributions

Key features and contributions of this work are as follows:

1) We present an analytical framework to mathematically capture the traffic-energy imbalances in a dual-powered cellular wireless network. Next, we apply this framework to leverage its effects through cooperative energy sharing, to improve the temporal network energy utilization without compromising the quality of service.
2) We first analyze the optimal solar provisioning required for the BSs in a non-networked, off-grid scenario. It is obtained statistically using the Parzen-window kernel density estimation technique, in accordance with the energy harvest and traffic profile.
3) A networked energy sharing framework is designed and optimized independently from two perspectives, namely, carbon emission-centric and operator revenue-centric. Carbon footprint reduction viewpoint aims at eliminating the need of grid energy procurement; the surplus energy is sold to the power grid as 'energy producer'. The operator revenue ('energy prosumer') maximization viewpoint involves the flexibility of energy procurement from the power grid in addition to energy selling and cooperative energy sharing.
4) Both the perspectives are mathematically formulated as a convex optimization problem for a given CAPEX and are independently optimized to estimate the optimal values. Optimal CAPEX and operator net revenue are calculated using a linear optimization framework for the two proposed modes of network operation.
5) As demonstrated via simulations, the proposed cooperative energy framework significantly improves the utilization of temporal network energy and reduces the grid energy procurement, thereby providing significant revenue gains compared to the state-of-art energy management frameworks.

C. Organization

The organization of this paper is as follows. Section II introduces the system model of the framework. In Section III, we compute the optimal CAPEX in a non-networked off-grid scenario. In Section IV we invoke power grid connectivity and propose the networked energy cooperation based framework. Section V presents the results and inferences. Section VI concludes the paper.

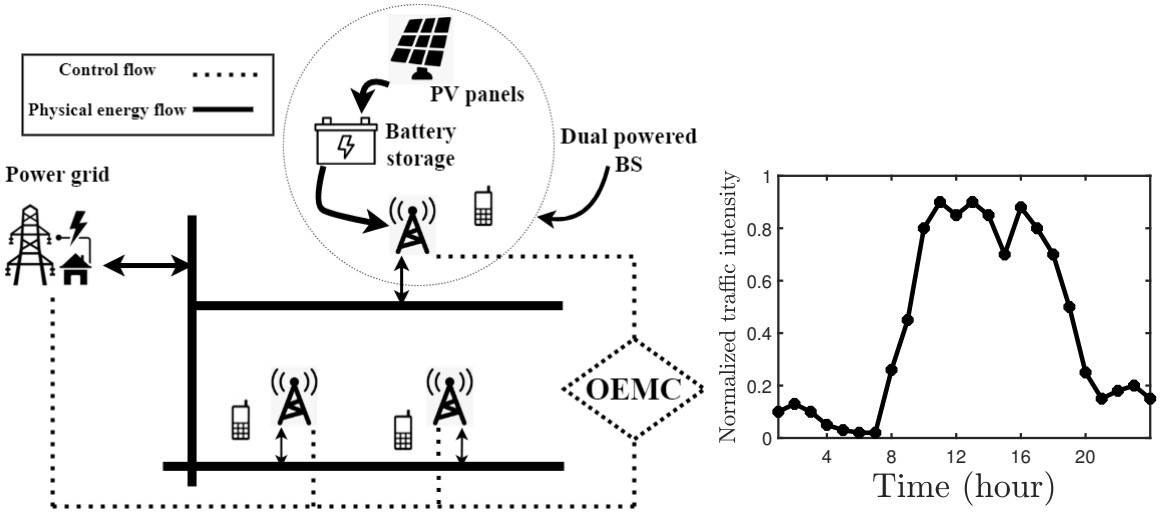

(a) Proposed dual-powered multi BS system model (b) Net traffic intensity over a day [25]

Figure 1: Illustration of the proposed system model and net traffic profile.

II. System Model

In this paper, we analyze the downlink of a dual-powered wireless communication network, subjected to skewed user traffic. Each BS is assumed to be equipped with a set of photovoltaic (PV) panels and battery storage of finite capacity. It is assumed that each dual-powered BS is connected with the power grid through an Operations and Energy Management Center (OEMC), which is implemented by the network operator at the core network as shown in Fig. 1(a). The OEMC communicates with the BSs using high capacity wired backhaul links. We consider a localized closed area $\mathcal{A}$, having $\mathcal{U}$ users following a homogeneous binomial point process of density λ_u, such that the users can displace within the area and not move out of it. Let the considered closed area $\mathcal{A}$ be covered by $\mathfrak{B}$ dual-powered BSs, having coverage radius $R_b \ \forall \ b \in \mathfrak{B}$. *K-means clustering* is used to compute the optimal BS coordinates in the area $\mathcal{A}$ using the user location coordinates. The downlink transmit power level of each BS is constrained to be between $0 \leq \mathcal{P}_b(t) \leq \mathcal{P}_m \ \forall \ b \in \mathfrak{B}$. In the upcoming subsections we will discuss the traffic profile, energy harvest profile, and resource allocation in the system.

A. Traffic profile

Let the hourly varying net traffic intensity over the area $\mathcal{A}$ under consideration be represented as $\rho(t)$. This net traffic profile shown in Fig. 1(b) has been taken from [25]. Further, the BSs are considered to be subjected to skewed user traffic, such that at any given hour of the day, any one BS is subjected to user traffic of greater intensity than the others. Hence, skewness in traffic refers to the degree of traffic inhomogeneity subjected upon a BS relative to other BSs [13], [26], [27]. Let the user traffic experienced at each BS be represented as $\rho_b(t) \ \forall \ b \in \mathfrak{B}$, such that $\sum_{b=1}^{\mathfrak{B}} \rho_b(t) = \rho(t)$. The skewed traffic profile is mathematically modelled as,

$$\psi_b(t) = \frac{e^{\zeta b}}{\sum_{b=1}^{\mathfrak{B}} e^{\zeta b}}, \text{s.t.,} \ \sum_{b=1}^{\mathfrak{B}} \psi_b(t) = \sum_{b=1}^{\mathfrak{B}} \frac{e^{\zeta b}}{\sum_{b=1}^{\mathfrak{B}} e^{\zeta b}} = 1. \tag{1}$$

Here, ζ represents the traffic-skewness intensity factor. Further, the traffic experienced at each BS is computed as $\rho_b(t) = \psi_b(t) \times \rho(t)$, with the number of active users associated with the BS being $\mathcal{U}_b(t) = \mathcal{U} \times \rho_b(t)$. We illustrate the effect of skewness factor ζ on the traffic experienced by the BSs in Fig. 2(a). For simulation purposes, we consider that a cluster of seven BSs covers the area under observation. In Fig. 2(a) we vary ζ between $[0, 3]$ and illustrate the variation of skewed traffic experienced at each BS of the network. It is notable that $\zeta = 0$ corresponds to the homogeneous traffic scenario wherein all the BSs experience equal average traffic. Increasing ζ relates to increasing the traffic inhomogeneity in the network. For instance, at an increased $\zeta = 3$, we observe that one BS experiences up to 95% of the net traffic at that instant while the other BSs experience negligible traffic.

The concept of spatio-temporally varying traffic imbalances is illustrated in Figs. 2(b) and 2(c). Fig. 2(b) depicts the variation of skewed traffic upon the BSs at $\zeta = 0.3$, while Fig. 2(c) showcases the variation of skewed traffic upon the BSs at $\zeta = 1.2$. In this paper, for numerical results and comparison purposes, we consider the area $\mathcal{A}$ to be covered by seven dual-powered BSs. The values of ζ considered along with the corresponding fraction of traffic intensity experienced by the BSs at any random hour are shown in Table I. To ensure that all the BSs experience skewed traffic, we include all possible permutations of these skewness levels in our analysis.

B. Energy harvesting profile

Each dual-powered BS is assumed to be equipped with $\mathcal{N}_{PV}$ PV panels and η_B batteries each having a capacity $\mathbb{B}_c$, for energy storage. Let, $\mathcal{H}_b(t)$ be the solar energy harvested at BS b through the equipped PV panels. We have obtained the annual hourly energy harvest data by a unit rated PV panel from National Renewable Energy Laboratory [28]. This energy is stored in the battery having a maximum storage capacity $\beta_m = \eta_B \mathbb{B}_c$. The battery also has a critical level below which it will not discharge, which is represented as $\beta_c = \delta \eta_B \mathbb{B}_c$. Here, δ represents the depth of discharge chosen

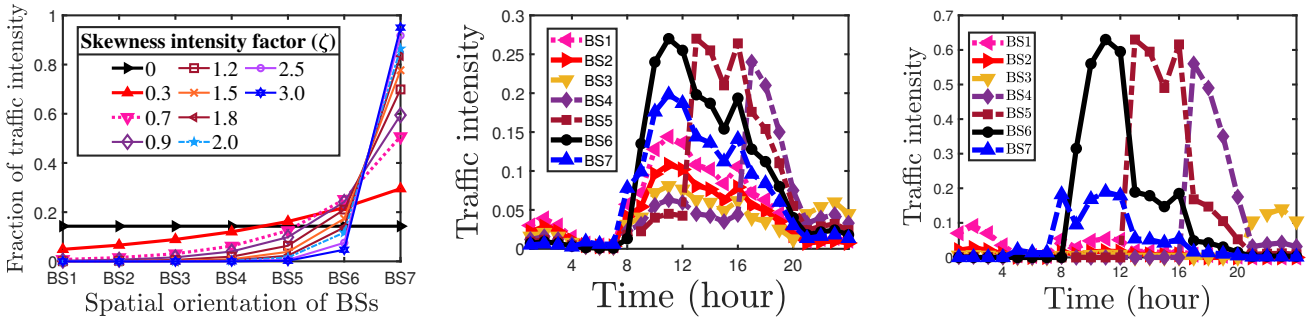

(a) (b) (c)

Figure 2: (a) Variation of BS traffic intensity at any hour, (b) Spatio-temporal variation of skewness $\zeta = 0.3$, (c) Spatio-temporal variation of skewness $\zeta = 1.2$.

Table I: Traffic skewness variation in BSs at any hour

ζ	BS7(%)	BS6(%)	BS5(%)	BS4(%)	BS3(%)	BS2(%)	BS1(%)
0	14.28	14.28	14.28	14.28	14.28	14.28	14.28
0.3	29.53	21.88	16.20	12.00	08.89	06.59	04.88
0.7	50.71	25.18	12.50	06.21	03.08	01.53	0.76
0.9	59.45	24.17	09.82	03.99	01.62	0.66	0.26
1.2	69.89	21.05	06.34	01.90	0.57	0.17	0.05
1.5	77.68	17.33	03.86	0.86	0.19	0.04	9.5×10^{-3}
2.0	86.46	11.70	1.58	0.21	0.029	3.92×10^{-3}	5.31×10^{-4}
3.0	95.02	4.73	0.23	0.011	5.83×10^{-4}	2.96×10^{-5}	1.44×10^{-6}

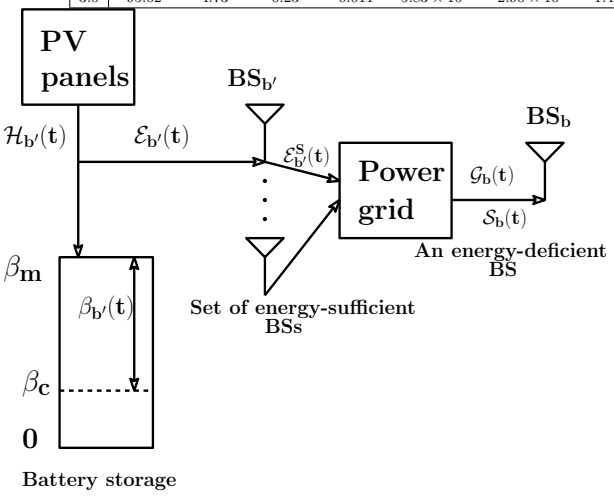

Figure 3: Energy flow in proposed model.

by the mobile network operator. Depending on the hourly BS energy consumption $\mathcal{E}_b(t)$ and the hourly BS solar harvest $\mathcal{H}_b(t)$, the battery level at each BS b is computed as

$$\begin{aligned} \beta'_b(t) &= \beta_b(t-1) + \mathcal{H}_b(t) - \mathcal{E}_b(t) \\ \beta_b(t) &= \min\left\{\max\left\{\beta'_b, \beta_c\right\}, \beta_m\right\}. \end{aligned} \tag{2}$$

This energy flow in a dual-powered network is represented in Fig. 3. Depending on the hourly battery level, a BS is classified as energy deficient, or energy sufficient (indexed by b'). A BS will be *energy deficient* if $\beta'_b(t) < \beta_c$. In this case, the amount of deficient energy required at BS b to avoid energy outage will be $\mathcal{D}_b(t) := (\beta_c - \beta'_b(t))$. In case a BS is *energy sufficient*, i.e., $\beta'_{b'}(t) > \beta_c$, the amount of sharable energy by BS b' is then defined as $\mathcal{E}^S_{b'}(t) := (\beta'_{b'}(t) - \beta_c)$.

C. Resource allocation and power profile

It is assumed that all the BSs in the network get access to the frequency spectrum depending on the fraction of users associated with them. Let the total frequency resource available be BW. Depending on the traffic load at each BS $\rho_b(t)$, frequency resource allocated to each BS b will be $BW_b(t) = BW \times \rho_b(t)$. It is further assumed that each active user $u \in \mathcal{U}_b$ associated with a BS b is allocated an equal share of separate frequency resource, $BW_{ub}(t) = BW_b(t)/\mathcal{U}_b(t)\ \forall\ b \in \mathfrak{B}$. Thus, the data rate achievable by a BS b to an associated active user u present at a distance d_{ub} will be $r_{ub} = BW_{ub}(t)\log_2\left(1 + \text{SNR}_{ub}(t)\right)$. $\text{SNR}_{ub}(t)$ represents the signal-to-noise-ratio at user u when associated with BS b, and is given as

$$\text{SNR}_{ub}(t) = \frac{\mathcal{P}_{ub}(t) g_{ub}(t)}{(BW_{ub}\ \sigma^2)\, d^2_{ub}}. \tag{3}$$

Here $\mathcal{P}_{ub}(t)$ refers to the dynamic power allocated to user u, $g_{ub}(t)$ refers to the corresponding channel gain, and σ^2 refers to the power spectral density (PSD) of the additive white gaussian noise (AWGN).

Assuming that all the active users have the same quality of service (QoS) mandates from their corresponding BS, the user QoS requirements can be expressed as $\mathbb{P}\left(r_{ub}(t) \geq r_0\right) \geq p_0$. Here, r_0 represents the user QoS rate guarantee and $(1 - p_0)$ represents the outage probability. Considering the channel to be Rayleigh distributed and the corresponding channel gain exponential distributed with unit mean, the power profile of a BS b can be computed as

$$\begin{aligned} &\mathbb{P}\left(g_{ub} \geq \frac{\left[e^{(r_0 \ln 2/BW_{ub})} - 1\right] d^2_{ub}\left(BW_{ub}\ \sigma^2\right)}{\mathcal{P}_{ub}(t)}\right) \geq p_0 \\ &\text{or, } \exp\left(-\frac{\left[e^{(r_0 \ln 2/BW_{ub})} - 1\right] d^2_{ub}\left(BW_{ub}\ \sigma^2\right)}{\mathcal{P}_{ub}(t)}\right) \geq p_0 \end{aligned} \tag{4}$$

$$\text{which yields, } \mathcal{P}_{ub}(t) \geq \frac{\left[e^{(r_0 \ln 2/BW_{ub})} - 1\right] d^2_{ub}\left(BW_{ub}\ \sigma^2\right)}{\ln(1/p_0)}. \tag{5}$$

Expression (5) represents the power required for a user u as a function of its distance d_{ub} from the BS b. Since the users are distributed following a binomial point process, the user locations with the BS at the center follow exponential distribution. The corresponding probability density function (PDF) is given as $f_Y(y) = 2\pi\lambda_u y\ e^{-\lambda_u \pi y^2}$ [14]. Thus, the

hourly average BS transmit power level is computed as

$$\mathcal{P}_b = \int_0^{R_b} \mathcal{P}_{ub}(y) f_Y(y) dy = \frac{\left[1 - e^{(r_0 \ln 2 \ \mathcal{U}_b / BW_b)}\right] \sigma^2 e^{-\lambda_u \pi R_b^2} BW_b}{\ln(p_0) \ \mathcal{U}_b} \left(R_b^2 + \frac{1}{\pi \lambda_u} \right). \quad (6)$$

Proof. Please refer to Appendix A. □

Depending on the computed dynamic hourly transmit power level $\mathcal{P}_b(t)$, the net energy consumed by a BS b is computed as

$$\mathcal{E}_b(t) = \mathcal{N}_{TRX}(\mathcal{P}_0 + \theta \mathcal{P}_b(t)). \quad (7)$$

Here, N_{TRX} represents the number of transceivers in the BS, $\mathcal{P}_0$ represents the static power consumed by the BS hardware, and θ represents the slope of dynamic power consumption [29]. The upcoming section presents the CAPEX computation in a non-networked, off-grid scenario.

III. Optimal CAPEX in an Off-Grid Non-Networked Scenario

As a benchmark case, we compute the optimal number of PV panels and storage batteries needed per BS, to make the system sustainable and free from energy outages in a non-networked scenario, where it is assumed that the BSs are not connected to the power grid. In the subsequent sections, we invoke the power grid connectivity when we discuss our proposed cooperative energy sharing framework.

A. Probability density estimation

CAPEX refers to the cost borne by the mobile operator to install the dual-powered network. It includes the cost involved in equipping the BSs with PV panels and battery storage capacity. In the current off-grid non-networked scenario, we mathematically model the system using the traffic and energy harvest profile. Since both traffic load and energy harvest are random in nature, we first compute the difference energy between the energy harvested and energy required to serve the BS traffic load at each BS $b \in \mathfrak{B}$. This can be represented as

$$\mathbb{D}_b(t) = \mathcal{H}_b(t) - \mathcal{E}_b(t). \quad (8)$$

This difference energy $\mathbb{D}_b(t)$ represents a random variable capturing the stochasticity of both energy harvest and traffic load. The set of difference energies are stored in $\mathbf{D} = \{\mathbb{D}_b(t)\} \ \forall \ b \in \mathfrak{B} \ \& \ \forall \ t$. The corresponding histogram plot of $\mathbf{D}$ is captured and its PDF for various skewed traffic scenarios is shown in Fig. 4. We observe that the PDF takes positive as well as negative values of difference energy, $\mathbb{D}_b(t)$. Clearly, there is a finite probability of $\mathbb{D}_b(t)$ to be positive (indicating that $\mathcal{H}_b(t) \geq \mathcal{E}_b(t)$), and likewise, $\mathbb{D}_b(t)$ can also take negative values (indicating that $\mathcal{E}_b(t) > \mathcal{H}_b(t)$).

To ensure a sustainable off-grid system without any energy outage, the BS should be equipped with sufficient battery storage such that, when $\mathbb{D}_b(t)$ is negative, the BS gets the corresponding supply from its battery storage and does not go into outage.

We use kernel density estimation strategy with Gaussian kernel to estimate the underlying data distribution. This technique is also called as Parzen-Rosenblatt window technique [30]. The PDF estimate using Gaussian kernel Parzen window is represented as a sum of Gaussians and is shown below.

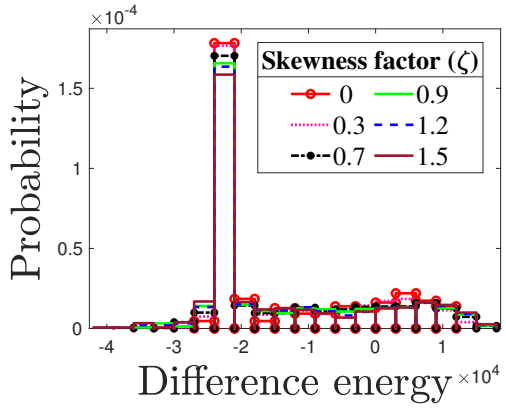

Figure 4: Variation of PDF with ζ.

$$\hat{f}_{\mathbb{D}}(d_0) = \frac{\sum_{j=1}^{|\mathbf{D}|} \mathbb{F}(d_0 - d_j, w)}{|\mathbf{D}|} = \frac{1}{|\mathbf{D}|} \sum_{j=1}^{|\mathbf{D}|} \frac{1}{(2\pi w^2)^{1/2}} e^{-(d_0 - d_j)^2 / 2w^2}. \quad (9)$$

Here, $|\mathbf{D}|$ refers to the cardinality of set $\mathbf{D}$, $\mathbb{F}$ refers to the weighting function or kernel function used in the estimation of density points, and w refers to the smoothing parameter or bandwidth of the kernel, which is used to control the window of observation samples for estimating the probability density at a new point.

We use mean square error (MSE) to measure the performance of the kernel based density estimation and to further compute the optimal Gaussian kernel bandwidth w. It is computed as shown below.

$$\text{MSE}(w) = \mathbb{E}\left[\left(\hat{f}_{\mathbb{D}}(d_0) - f_{\mathbb{D}}(d) \right)^2 \right]. \quad (10)$$

Here, $f_{\mathbb{D}}(d)$ represents the true density function, while $\hat{f}_{\mathbb{D}}(d_0)$ represents the estimated density function. The optimal kernel bandwidth is chosen by finding the argument that minimizes the above defined MSE function. This is shown as

$$w^* = \arg\min_w \text{MSE}(w) \quad \text{s.t. } w \geq 0. \quad (11)$$

B. Optimal CAPEX computation

To compute the optimal CAPEX in such an off-grid non-networked scenario, we use the analytical expression of PDF of the difference energy, obtained in the previous subsection. It may be noted that the PDF represented in (9) accounts for the daily fluctuations in solar energy harvest as well as the load demand (shown in Fig. 4). The PDF effectively captures the temporal stochasticity of difference energy arising due to randomness in harvest energy and load demand profile. The minimum number of solar panels to be provisioned with a BS should satisfy $\mathbb{E}[\mathbb{D}_b(t)] \geq 0$, or $\mathbb{E}[\mathcal{H}_b(t)] \geq \mathbb{E}[\mathcal{E}_b(t)]$ in a long run. For a system having PV panels of rating $\mathcal{R}$ kW and a lifetime of $\mathcal{L}_{PV}$, the minimum number of PV panels to be

provisioned with each BS for a duration of $\mathcal{Y}$ years will be

$$\mathcal{N}_{PV}^{O} \geq \frac{\mathbb{E}[\mathbb{D}]}{\mathfrak{B} \times \mathcal{R}} \left(\frac{\mathcal{Y}}{\mathcal{L}_{PV}} \right). \tag{12}$$

It is notable that, since we are statistically estimating the solar provisioning based on the annual hourly solar irradiance data obtained from [28], the number of PV panels is estimated such that energy neutrality is maintained. Hence, the expectation of the difference energy should remain positive.

Further, we observe that the difference energy can be both positive as well as negative. While dimensioning the storage capacity of a BS, it should be ensured that when the energy harvest at any hour is less than the BS load (i.e., difference energy is negative), the BS storage should ensure smooth operation of the BS without energy outage. Thus, the battery storage capacity $\mathbb{C}$ is defined as

$$\mathbb{C} \geq \int_{-\infty}^{0} d_0 \hat{f}_{\mathbb{D}}(d_0) d(d_0). \tag{13}$$

Taking the battery depth of discharge δ into consideration, the optimal number of storage batteries η_B^O of capacity $\mathcal{B}_c$, having a lifetime $\mathcal{L}_B$ to be equipped with each BS is computed as

$$\eta_B^O \geq \frac{\mathbb{C}}{(1-\delta) \times \mathcal{B}_c \times \mathfrak{B}} \left(\frac{\mathcal{Y}}{\mathcal{L}_B} \right). \tag{14}$$

The corresponding CAPEX incurred to the operator is computed as

$$CAPEX^O = \left(c_{PV} \mathcal{N}_{PV}^O + c_B \eta_B^O \right) \mathfrak{B}, \tag{15}$$

where c_{PV} and c_B represent the cost of a unit rated PV panel and battery respectively. The life expectancy of PV panels is generally constant [31], whereas the life expectancy of a battery is dependent on the number of charging-discharging cycles and the depth of discharge set by the operator. Battery lifetime $\mathcal{L}_B$ is computed using the framework in [32], which accounts for the number of charging-discharging cycles, operating temperature T_c (in Celsius), and depth of discharge δ. The dependence of battery cycles $\mathcal{C}$, on T_c and δ is given as

$$\mathcal{C}(\delta, T_c) = \mathcal{C}(\delta) \times (37.38 \times T_c^{-1.101} - 0.3897). \tag{16}$$

Further, the battery lifetime $\mathcal{L}_B$ is computed as

$$\mathcal{L}_B = \frac{1}{\sum_{k=1}^{\mathcal{C}(\delta)} \frac{1}{\mathcal{C}(\delta, T_c)}}. \tag{17}$$

In the upcoming section we invoke the power grid connectivity and observe the effect of networked operation on grid energy procurement and operator revenue.

IV. Grid Connected Networked Energy Cooperation based Framework

This section proposes analytical approaches to study power grid connected energy cooperation in dual-powered networks. It is assumed that the solar-enabled BSs have the flexibility to procure or sell energy to the power grid, in addition to cooperative transfer of energy among the networked BSs via the grid infrastructure itself.

A. Grid energy procurement minimization

We begin the analysis of a networked dual-powered network by formulating a grid energy procurement minimization problem. For a given CAPEX, the OEMC classifies the BSs at each hour into two disjoint sets as *energy deficient* or *energy sufficient*, as discussed in Section II-B. Let I out of $\mathcal{B}$ BSs be energy deficient at a given hour, and the remaining $J = (\mathcal{B} - I)$ BSs be energy sufficient. For the I energy deficient BSs, the net hourly deficit energy is

$$\mathcal{D}(t) = \sum_{b=1}^{I} \mathcal{D}_b(t) = \sum_{b=1}^{I} \left(\beta_c - \beta_b'(t) \right). \tag{18}$$

For the remaining J energy sufficient BSs, the hourly net sharable energy available in the network is

$$\mathcal{E}^S(t) = \sum_{b'=1}^{J} \mathcal{E}_{b'}^S(t) = \sum_{b'=1}^{J} \left(\beta_{b'}(t) - \beta_c \right). \tag{19}$$

In the proposed energy sharing framework, an energy deficient BS can meet its deficit energy requirement in two ways. The energy deficient BS either receives the deficit energy by cooperative energy transfer through the energy sufficient BSs or by energy procurement through the power grid. We define $\mathcal{S}_b(t)$ as the portion of deficit energy coming from the J energy sufficient BSs to an energy deficient BS b and $\mathcal{G}_b(t) = (\mathcal{D}_b(t) - \mathcal{S}_b(t))$ as the remaining portion of deficit energy being procured from the power grid by the deficient BS b.

We aim to minimize the grid procurement $\mathcal{G}_b(t) \geq 0$ at each BS, i.e., $\min\ \mathcal{G}_b(t)$. Since, $\mathcal{G}_b(t) = (\mathcal{D}_b(t) - \mathcal{S}_b(t))$, hence $\min\ \mathcal{G}_b(t) \equiv \max\ \mathcal{S}_b(t)$. Ideally for minimizing the grid energy procurement, i.e., for achieving $\mathcal{G}_b(t) = 0$, $\mathcal{S}_b(t) = \mathcal{D}_b(t)$. Hence, from the network perspective,

$$\sum_{b=1}^{I} \mathcal{S}_b(t) = \min \left\{ \sum_{b'=1}^{J} \mathcal{E}_{b'}^S(t), \sum_{b=1}^{I} \mathcal{D}_b(t) \right\} \tag{20}$$

and

$$0 \leq \sum_{b=1}^{I} \mathcal{S}_b(t) \leq \sum_{b=1}^{I} \mathcal{D}_b(t). \tag{21}$$

The corresponding grid energy minimization problem formulation is defined as

$$\begin{aligned} \mathcal{P}1: \ & \max_{\mathcal{S}_b} \sum_{b=1}^{I} \mathcal{S}_b(t) \\ \text{s.t. } & 0 \leq \sum_{b=1}^{I} \mathcal{S}_b(t) \leq \sum_{b=1}^{I} \mathcal{D}_b(t) \\ & \sum_{b=1}^{I} \mathcal{S}_b(t) = \min \left\{ \sum_{b'=1}^{J} \mathcal{E}_{b'}^S(t), \sum_{b=1}^{I} \mathcal{D}_b(t) \right\}. \end{aligned} \tag{22}$$

The problem $\mathcal{P}1$ is observed to be a single variable linear optimization problem with affine and concave constraints. However, it can be observed that the decision variable $\mathcal{S}_b(t)$ vanishes on differentiation. Since we aim to find the optimal amount of energies which can be shared (or procured) to (or by) an energy deficit BS, i.e., we need to find the optimum

value of $\mathcal{S}_b(t)$, $\mathcal{P}1$ is reformulated as a quadratic convex problem $\mathcal{P}2$, shown below, in order to derive closed-form results and make the problem mathematically tractable.

$$\begin{aligned} \mathcal{P}2: &\max_{\mathcal{S}_b} \sum_{b=1}^{I} \left(\mathcal{S}_b(t)\right)^2 \\ \text{s.t. } C1: &\sum_{b=1}^{I} \mathcal{S}_b(t) \leq \sum_{b=1}^{I} \mathcal{D}_b(t) \\ C2: &\sum_{b=1}^{I} \mathcal{S}_b(t) = \min\left\{\sum_{b'=1}^{J} \mathcal{E}_{b'}^{S}(t), \sum_{b=1}^{I} \mathcal{D}_b(t)\right\} \\ C3: &\sum_{b=1}^{I} \mathcal{S}_b(t) \geq 0. \end{aligned} \tag{23}$$

We observe that $\mathcal{P}2$ is a purely convex optimization problem. This is because the objective function is convex in nature, constraints C1 and C3 are affine, while constraint C2 is concave in nature.

Lemma 1. *For a dual-powered network consisting of $\mathfrak{B}$ BSs, the minimum power grid energy procurement required by an energy deficient BS b is*

$$\mathcal{G}_b(t) = \begin{cases} 0, \text{ if } \sum_{b=1}^{I} \mathcal{D}_b(t) \leq \sum_{b'=1}^{J} \mathcal{E}_{b'}^{S}(t) \\ \mathcal{D}_b(t)\left(\frac{\sum_{b=1}^{I} \mathcal{D}_b(t) - \sum_{b'=1}^{J} \mathcal{E}_{b'}^{S}(t)}{\sum_{b=1}^{I} \mathcal{D}_b(t)}\right), \\ \qquad \text{if } \sum_{b'=1}^{J} \mathcal{E}_{b'}^{S}(t) < \sum_{b=1}^{I} \mathcal{D}_b(t). \end{cases} \tag{24}$$

and the maximum energy that can be shared to a energy deficient BS is given as

$$\mathcal{S}_b(t) = \begin{cases} \mathcal{D}_b(t), \text{ if } \sum_{b=1}^{I} \mathcal{D}_b(t) \leq \sum_{b'=1}^{J} \mathcal{E}_{b'}^{S}(t) \\ \left(\mathcal{D}_b(t) \sum_{b'=1}^{J} \mathcal{E}_{b'}^{S}(t)\right) / \sum_{b=1}^{I} \mathcal{D}_b(t), \\ \qquad \text{if } \sum_{b'=1}^{J} \mathcal{E}_{b'}^{S}(t) < \sum_{b=1}^{I} \mathcal{D}_b(t). \end{cases} \tag{25}$$

Proof. Please refer to Appendix B. □

Expression (25) is the optimal solution of $\mathcal{P}2$. From (24) and (25) it can be inferred that there is no temporal grid energy procurement, i.e., $\mathcal{G}_b(t) = 0$, if $\sum_{b=1}^{I} \mathcal{D}_b(t) \leq \sum_{b'=1}^{J} \mathcal{E}_{b'}^{S}(t)$. Also in this case the net energy shared to an energy-deficit BS equals the temporal deficit energy, i.e., $\mathcal{S}_b(t) = \mathcal{D}_b(t)$. Further, for the scenario when $\sum_{b'=1}^{J} \mathcal{E}_{b'}^{S}(t) < \sum_{b=1}^{I} \mathcal{D}_b(t)$, it is inferred that the deficit BSs get proportional share of energy as $\sum_{b'=1}^{J} \mathcal{E}_{b'}^{S}(t) / \sum_{b=1}^{I} \mathcal{D}_b(t)$.

B. Operator revenue maximization

In this subsection, we carry forward our analysis of networked dual-powered cellular BSs and formulate an analytical framework to maximize the operator revenue. Before delineating the analytical framework, we discuss the cost metrics associated with the system design. These metrics are listed below.

1) *CAPEX:* CAPEX involves the cost to be borne by the mobile network operator in solar provisioning the BSs. This is computed by taking into account the life expectancy of the PV panels and storage batteries. Considering a PV panel having a life expectancy $\mathcal{L}_{PV}$ and a storage battery having a life expectancy $\mathcal{L}_B$, CAPEX for $\mathcal{Y}$ years is computed as

$$CAPEX = \mathfrak{B}\left(\frac{c_{PV}\mathcal{N}_{PV}}{\mathcal{L}_{PV}} + \frac{c_B \eta_B}{\mathcal{L}_B}\right)\mathcal{Y}. \tag{26}$$

2) *Operational expenditure (OPEX):* In a networked operation scenario, OPEX relates to the cost incurred by the operator in procuring energy from the power grid and in cooperatively sharing energy amongst the BSs using the power grid infrastructure. They are defined below.

   a) *Energy sharing cost ($\mathcal{C}_{share}$):* This cost can also be perceived as a grid maintenance cost borne by the operator. We use the optimum energy to be shared by an energy sufficient BS (25) to compute $\mathcal{C}_{share}$ as defined below.

$$\mathcal{C}_{share} = \sum_{t=1}^{24} C_{sh} \times \sum_{b=1}^{I} \mathcal{S}_b(t). \tag{27}$$

   Here, C_{sh} refers to the cost of sharing unit energy by the sufficient BSs to deficit BSs, using the power grid infrastructure. This expenditure is proposed to be borne by the deficit BSs towards power grid maintenance. It is proposed that C_{sh} be less than the cost of unit grid energy procurement and the cost of selling unit energy back to the power grid, in order to incentivize the power grid operator for energy sharing rather than selling energy.

   b) *Grid energy procurement cost ($\mathcal{C}_{buy}$):* It refers to the cost incurred by the network operator in procuring energy from the power grid. It is computed as

$$\mathcal{C}_{buy} = \sum_{t=1}^{24} C_b \times \sum_{b=1}^{I} \mathcal{G}_b(t). \tag{28}$$

   Here, C_b refers to the cost of procuring unit energy from the power grid. Further, the net OPEX incurred to the operator is given as

$$OPEX = \mathcal{C}_{buy} + \mathcal{C}_{share}. \tag{29}$$

3) *Revenue earned by selling energy ($\mathcal{R}_{sell}$):* This is defined as the revenue earned by mobile operator through selling energy back to the power grid. The amount of energy that the operator can sell and earn revenue is given as

$$\begin{aligned} \sum_{b'=1}^{J} \mathcal{E}_{b'}^{R}(t) = &\sum_{b'=1}^{J} \mathcal{E}_{b'}^{S} - \sum_{b=1}^{I} \mathcal{D}_b(t), \\ &\text{iff } \sum_{b'=1}^{J} \mathcal{E}_{b'}^{S}(t) > \sum_{b=1}^{I} \mathcal{D}_b(t). \end{aligned} \tag{30}$$

Also we observe that,

$$\sum_{b=1}^{I} \mathcal{S}_b(t) = \min\left\{\sum_{b'=1}^{J} \mathcal{E}_{b'}^{S}(t), \sum_{b=1}^{I} \mathcal{D}_b(t)\right\}.$$

Thus, for $\sum_{b'=1}^{J} \mathcal{E}_{b'}^{S}(t) > \sum_{b=1}^{I} \mathcal{D}_b(t)$, the amount of

energy to be sold can be expressed as,

$$\sum_{b'=1}^{J} \mathcal{E}_{b'}^{R}(t) = \sum_{b'=1}^{J} \mathcal{E}_{b'}^{S}(t) - \sum_{b=1}^{I} \mathcal{S}_b(t). \tag{31}$$

Hence, $\mathcal{R}_{sell}$ is mathematically computed as

$$\begin{aligned} \mathcal{R}_{sell} &= \sum_{t=1}^{24} C_{se} \times \sum_{b'=1}^{J} \mathcal{E}_{b'}^{R}(t) \\ &= \sum_{t=1}^{24} C_{se} \left(\sum_{b'=1}^{J} \mathcal{E}_{b'}^{S}(t) - \sum_{b=1}^{I} \mathcal{S}_b(t) \right), \end{aligned} \tag{32}$$

with C_{se} referring to the cost of selling unit energy back to the power grid.

4) *Revenue earned by serving users* ($\mathcal{R}_{serv}$)*:* It refers to the revenue earned by the mobile operator through serving users. It is computed as

$$\mathcal{R}_{serv} = \sum_{b=1}^{\mathfrak{B}} \sum_{t=1}^{24} C_r \times \mathcal{U}_b(t). \tag{33}$$

Here, C_r [33] refers to the per-day revenue earned by the mobile operator by serving a user.

In accordance with the cost metrics discussed above, the annual net revenue $\mathcal{R}_o$ earned by the mobile operator in a dual-powered framework is computed as shown below.

$$\mathcal{R}_o = \mathcal{R}_{serv} + \mathcal{R}_{sell} - \mathcal{C}_{share} - \mathcal{C}_{buy} - CAPEX. \tag{34}$$

With $\mathcal{R}_{serv}$ being constant for a given skewness factor, the revenue maximization problem at a given CAPEX can be formulated as,

$$\begin{aligned} &\mathcal{P}3 : \max_{\mathcal{E}_{b'}^{R}, \mathcal{S}_b, \mathcal{G}_b} \left(C_{se} \sum_{b'=1}^{J} \mathcal{E}_{b'}^{R}(t) - C_{sh} \sum_{b=1}^{I} \mathcal{S}_b(t) - C_b \sum_{b=1}^{I} \mathcal{G}_b(t) \right) \\ &\text{s.t. } C1 : \sum_{b=1}^{I} \mathcal{S}_b(t) \leq \sum_{b=1}^{I} \mathcal{D}_b(t) \\ &C2 : \sum_{b=1}^{I} \mathcal{S}_b(t) < \min \left\{ \sum_{b'=1}^{J} \mathcal{E}_{b'}^{S}(t), \sum_{b=1}^{I} \mathcal{D}_b(t) \right\} \\ &C3 : \sum_{b=1}^{I} \mathcal{S}_b(t) \geq 0 \\ &C4 : \sum_{b=1}^{I} \mathcal{G}_b(t) = \sum_{b=1}^{I} \mathcal{D}_b(t) - \sum_{b=1}^{I} \mathcal{S}_b(t) \\ &C5 : \sum_{b'=1}^{J} \mathcal{E}_{b'}^{R}(t) = \sum_{b'=1}^{J} \mathcal{E}_{b'}^{S}(t) - \sum_{b=1}^{I} \mathcal{S}_b(t) \\ &C6 : \sum_{b'=1}^{J} C_{se} \mathcal{E}_{b'}^{R}(t) \geq 0. \end{aligned} \tag{35}$$

We observe that the problem $\mathcal{P}3$ has three decision variables, $\mathcal{E}_{b'}^{R}, \mathcal{S}_b, \mathcal{G}_b$. Also, we observe that constraint $C1 \subset C2$, thus eliminating $C1$.

For $\sum_{b=1}^{J} \mathcal{E}_b^S(t) > \sum_{b=1}^{I} \mathcal{D}_b(t)$, the amount of energy which can be sold back to the grid can be expressed in terms of $\mathcal{S}_b(t)$ through $C5$. Similarly, the network grid energy procurement $\sum_{b=1}^{I} \mathcal{G}_b(t)$ can be expressed in terms of $\sum_{b=1}^{I} \mathcal{S}_b(t)$ through $C4$. Therefore, we convert a three variable problem $\mathcal{P}3$ into a single variable problem $\mathcal{P}4$ as

$$\begin{aligned} \mathcal{P}4 : \max_{\mathcal{S}_b} \Bigg(& C_{se} \left(\sum_{b=1}^{J} \mathcal{E}_b^S - \sum_{b=1}^{I} \mathcal{S}_b(t) \right) - C_{sh} \sum_{b=1}^{I} \mathcal{S}_b(t) \\ & - C_b \left(\sum_{b=1}^{I} \mathcal{D}_b(t) - \sum_{b=1}^{I} \mathcal{S}_b(t) \right) \Bigg) \\ = \max_{\mathcal{S}_b} \Bigg(& (C_b - C_{se} - C_{sh}) \sum_{b=1}^{I} \mathcal{S}_b(t) + C_{se} \sum_{b=1}^{J} \mathcal{E}_b^S - C_b \sum_{b=1}^{I} \mathcal{D}_b(t) \Bigg). \end{aligned} \tag{36}$$

Again, in order to derive closed form expressions and to make the problem mathematically tractable, we revise the problem formulated in (36) by squaring the terms. Also, since this formulation is at a given hour t, we remove t from the formulation. The revised convex problem formulation $\mathcal{P}5$ is shown below.

$$\begin{aligned} &\mathcal{P}5 : \max_{\mathcal{S}_b} \left((C_b - C_{se} - C_{sh})^2 \sum_{b=1}^{I} (\mathcal{S}_b)^2 + \underbrace{C_{se}^2 \sum_{b=1}^{J} \left(\mathcal{E}_b^S\right)^2 - C_b^2}_{\text{constant, } \kappa} \right) \\ &\text{s.t. } C1 : \sum_{b=1}^{I} \mathcal{S}_b < \min \left\{ \sum_{b=1}^{J} \mathcal{E}_b^S, \sum_{b=1}^{I} \mathcal{D}_b \right\} \\ &\quad C2 : \sum_{b=1}^{I} \mathcal{S}_b \geq 0. \end{aligned} \tag{37}$$

$\mathcal{P}5$ is a convex problem as the objective function is convex, constraint C1 is concave, and constraint C2 is affine. The second and third terms of the above objective function are constant and independent of the decision variable $\mathcal{S}_b$ in an hour t and hence are expressed as a constant κ.

Theorem 1. *For a given CAPEX, the OPEX incurred in the grid energy procurement minimization problem is identical to the operator revenue maximization problem. That is, the solution of* $\mathcal{P}5$ *is*

$$\mathcal{S}_b(t) = \begin{cases} \mathcal{D}_b(t), \text{ if } \sum_{b=1}^{I} \mathcal{D}_b(t) \leq \sum_{b'=1}^{J} \mathcal{E}_{b'}^{S}(t) \\ \left(\mathcal{D}_b(t) \sum_{b'=1}^{J} \mathcal{E}_{b'}^{S}(t) \right) / \sum_{b=1}^{I} \mathcal{D}_b(t), \\ \qquad \text{if } \sum_{b'=1}^{J} \mathcal{E}_{b'}^{S}(t) < \sum_{b=1}^{I} \mathcal{D}_b(t). \end{cases} \tag{38}$$

Proof. Please refer to Appendix C. □

Thus, we show that for a given CAPEX, the OPEX involved in the grid energy minimization and the operator revenue maximization are identical, i.e., minimizing the grid energy procurement is influenced by maximizing the energy sharing among the networked BSs, thus reducing the operational expenditure and hence maximizing the operator revenue.

In the upcoming subsection, we present a framework to compute the optimal CAPEX along with the corresponding operator revenue and propose two innovative strategies for network operation.

C. Optimal CAPEX in networked scenario

We present a linear optimization based framework to compute the optimal CAPEX and further the maximum revenue achievable to a mobile network operator. The problem of

computing the optimal CAPEX is decoupled into two sub-problems, first computing the optimal OPEX (and hence the corresponding operator revenue) for a given CAPEX (as performed in Section IV-B), then computing the optimal CAPEX based on the mode of network operation.

We first describe the two proposed modes of network operation. These strategies have been devised from the environmental perspective of reducing the carbon footprint (energy producer mode) and from the operator's perspective of maximizing revenue (energy prosumer mode).

1) Energy producer mode

The proposed carbon free energy producer mode of network operation involves the operator running the network such that the networked BSs act as a distributed energy producer to the power grid. In this mode of network operation, it is assumed that the BSs, without the flexibility to procure energy from the grid, can cooperatively share energy amongst each other and/or sell energy back to the power grid. Thus, in this mode while the BSs are connected to the power grid, they are powered only through green solar energy harvested in their battery storage.

2) Energy prosumer mode

The energy prosumer mode relates to the scenario wherein the networked BSs being dual-powered act as both, energy producers to the grid (i.e., sell energy to the grid) as well as energy consumers (i.e., procure energy from the grid). In this mode of network operation, the BSs in addition to energy procurement and selling, also have the flexibility to share energy amongst each other cooperatively.

Optimal CAPEX varies for both the proposed modes of network operation. For the energy producer mode, optimal CAPEX refers to the CAPEX at which the cellular network can operate without any grid energy procurement. For the energy prosumer mode, optimal CAPEX refers to the CAPEX at which the operator can earn maximum revenue.

We observe that $\mathcal{R}_{serv}$ is constant for a given traffic skewness and that energy selling ($\mathcal{R}_{sell}$) and operational expenditure costs (C_{share} and C_{buy}) are influenced by the CAPEX, i.e., they depend on the battery storage and energy harvesting capacity of the BS. In the previous subsections we computed the optimal revenue $\mathcal{R}_o$ for a given CAPEX. The problem now reduces to finding the optimal CAPEX at which the operator will earn maximum revenue $\mathcal{R}_o$. This problem evolves as a linear optimization problem as shown below,

$$\begin{aligned} \mathcal{P}6: \ & \max \ \mathcal{R}_o \\ \text{s.t. } & C1: CAPEX = \mathfrak{B}\left(\frac{c_{PV}\mathcal{N}_{PV}}{\mathcal{L}_{PV}} + \frac{c_B\eta_B}{\mathcal{L}_B}\right)\mathcal{Y} \\ & C2: \mathcal{N}_{PV} \geq 0 \\ & C3: \eta_B \geq 0 \\ & C4: CAPEX \leq CAPEX^O. \end{aligned} \tag{39}$$

Thus, an exhaustive search based linear optimization is performed in order to compute the optimal CAPEX depending on the operator's mode of operation. It may be noted that the optimal CAPEX expression derived in Section III, denoted as $CAPEX^O$, represents the upper limit of CAPEX which can be provisioned at a BS. Hence, $\mathcal{P}6$ is constrained by $C4$, thus reducing the search space of the linear optimization problem. The variation of operator revenue when the network operates at the proposed modes will be discussed in Section V-C.

Table II: Parameter values used in simulations along with description

$\mathcal{A}$	1 km^2	Area under observation
$\mathfrak{B}$	7	Number of BSs considered
λ_u	3000	User density
$\mathcal{P}_m$	40 W [29]	Maximum BS downlink transmit power level
$\mathbb{B}_c$	2460 Wh [32]	Battery capacity
δ	0.3 [32]	Depth of discharge
BW	20 MHz [35]	System bandwidth considered
σ^2	-150 dBm/Hz [37]	PSD of AWGN
r_0	300×10^3 bps [35]	User QoS
p_0	0.9 [39]	Non-outage probability
c_{PV}	1300 USD [34]	Cost of unit PV panel
c_B	216 USD [36]	Cost of unit storage battery
C_{sh}	0.015 USD	Price of sharing unit energy
C_b	0.079 USD [38]	Price of purchasing unit energy from power grid
C_{se}	0.057 USD [40]	Price of selling unit energy

V. Results

In this section we discuss the beneficial effects of cooperative networked operation in dual-powered cellular networks. We will discuss and compare the optimal CAPEX required to design the system, the reduction in grid energy procurement, and the operator revenue gains achieved through the proposed modes of network operation, with the state of art. The simulations have been performed in MATLAB 2020a. The parameter values considered in the simulations is shown in Table II.

A. Optimal CAPEX

In this subsection we illustrate the computation of optimal CAPEX in an off-grid non-networked scenario, and compare it with the CAPEX incurred in the proposed networked modes of operation. Through Fig. 5(a) we illustrate the Parzen window density estimation technique employed to compute the optimal CAPEX in an off-grid non networked scenario. Fig. 5(a) shows the true and estimated cumulative probability function (CDF) of the difference energy at $\zeta = 1.5$. It can be observed that the estimated CDF follows the true CDF very closely and results in an RMSE of 1.0956×10^{-4} shown in Table III. The values of optimal kernel bandwidth and the corresponding RMSE values between the estimated and true CDF for various skewed traffic scenarios are shown in Table III.

Through Fig. 5(b) we illustrate the variation of optimal CAPEX with an increase in traffic inhomogeneity for various modes of network operation. For the off-grid scenario, we observe that the CAPEX increases with an increase in traffic skewness up to $\zeta = 0.7$, peaking at \$83424. The CAPEX then reduces and saturates at around \$76072 with further increase in traffic inhomogeneity. In contrast to the off-grid scenario,

Table III: Variation of CAPEX estimation parameters with skewness

ζ	0	0.3	0.7	0.9	1.2	1.5
RMSE	1.2895×10^{-4}	1.2844×10^{-4}	1.2192×10^{-4}	1.661×10^{-4}	1.1408×10^{-4}	1.0956×10^{-4}
w^*	7.0774	7.0916	7.1647	7.2036	7.2588	7.3037

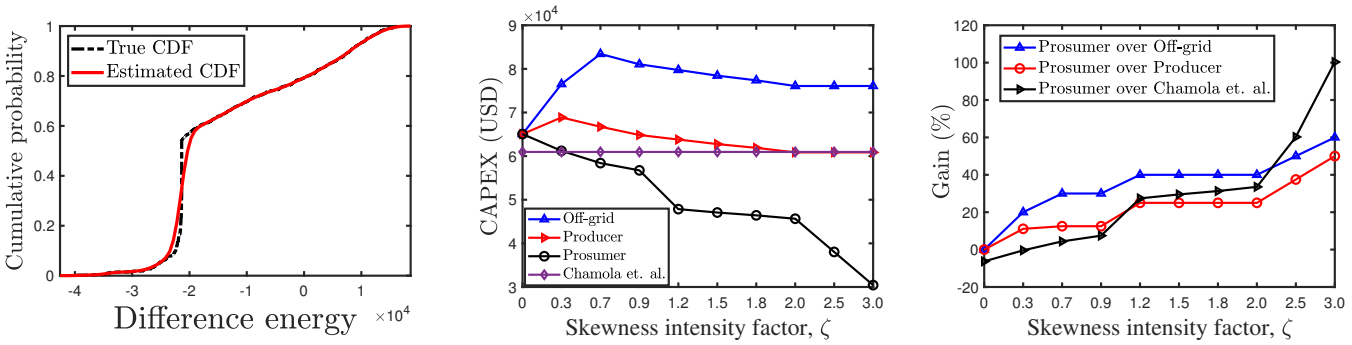

(a) (b) (c)

Figure 5: (a) Estimated and the true CDF, $\zeta = 1.5$, (b) Variation of optimal CAPEX with ζ, (c) CAPEX saving in prosumer mode.

we observe that the proposed energy producer and energy prosumer modes result in significant CAPEX saving to the network operator. It is observed that, in the homogeneous traffic condition (i.e., with $\zeta = 0$) all the three modes of network operation have equal CAPEX. Further, it is observed from Fig. 5(c) that the prosumer mode results in a CAPEX saving of about 60% over the off-grid mode of operation, and a saving of about 50% over the energy producer mode.

The optimal CAPEX considered in the dual-powered without energy sharing (WES) framework of [20] is constant. It can be inferred from Fig. 5(c) that for the balanced homogeneous traffic scenario, the prosumer mode achieves negative CAPEX gain over [20]. But with increasing traffic inhomogeneity, the prosumer mode offers significant CAPEX saving, achieving up to 100% gain. The reduced CAPEX with the networked modes of operation can be attributed to the improvement in the utilization of temporal network energy through the proposed cooperative energy sharing strategy among the BSs. Specifically, the energy prosumer mode is observed to incur lesser CAPEX to the operator than the energy producer mode. This is due to the fact that the energy producer mode being a carbon free mode of network operation incurs extra CAPEX as discussed later in Section V-C.

Remark 1. *Cooperative networked energy transfer among the BSs significantly reduces the CAPEX incurred by the operator over an off-grid non-networked scenario. The gain in CAPEX saving with the prosumer mode, significantly increases with increase in traffic heterogeneity.*

Remark 2. *The proposed energy prosumer mode results in lower CAPEX over the proposed energy producer mode of network operation.*

B. Reduction in grid procurement

In this subsection we illustrate the reduction in grid energy procurement achieved through the proposed prosumer mode of cooperative energy sharing framework. It may be noted that the proposed producer mode is already a carbon free mode and hence has not been shown.

In Fig. 6(a), as a baseline comparison, we have compared the grid energy procurement in the proposed prosumer mode with a dual-powered WES based framework considered in [20]. Additionally, to show the magnitude of reduction in carbon emissions, we also illustrate the grid energy procurement in a fully grid-powered system [14]. It can be observed that the prosumer mode of network operation results in a significantly lower grid energy procurement as compared to [20] and [14].

Fig. 6(b) shows the average reduction in grid energy procurement with increasing traffic inhomogeneity over [20]. We observe that the homogeneous traffic condition ($\zeta = 0$) does not involve any reduction in grid energy. This is essentially due to balanced loads on all the BSs in the network and same energy harvest assumed on all the BSs. Further it is observed that with increasing traffic skewness, the system is able to reduce up to 62.07% of its grid energy procurement (at $\zeta = 1.2$). The average grid energy procurement reduction is observed to decrease marginally after $\zeta = 1.2$, saturating at around 56%.

Remark 3. *Cooperative energy transfer results in significant reduction of grid energy procurement over a dual-powered WES based framework.*

Through Fig. 6(c), we illustrate the variation in grid energy procurement with increasing CAPEX for various skewed traffic scenarios. It may be noted that $CAPEX^O$ represents the optimal CAPEX required in the off-grid non-networked scenario, as discussed in Section III-B. We observe that when the system is subjected to homogeneous traffic, then the system is able to be carbon free only at full CAPEX (i.e., at $CAPEX^O$). The reduction in grid energy procurement at $\zeta = 0$ is attributed to increasing $CAPEX^O$, which eventually results in lowering the grid energy procurement. On the contrary, the proposed cooperative energy sharing framework

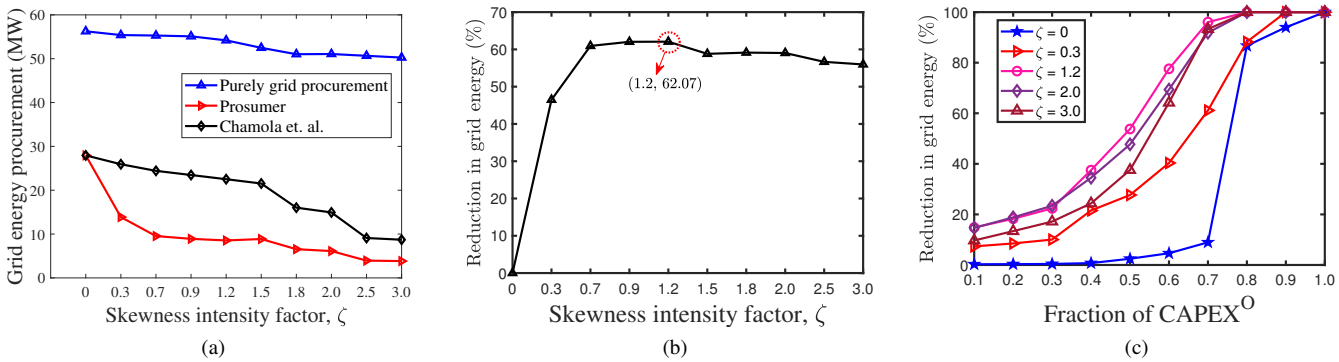

Figure 6: (a) Comparison of grid energy procurement in various modes of network operation, (b) Average reduction in grid procurement with ζ over [20], (c) Variation of grid reduction with CAPEX.

is advantageous with increasing traffic inhomogeneity. We observe that subjecting the system to skewed traffic ($\zeta > 0$) results in achieving self sustainable networks at a significantly lower CAPEX.

Remark 4. *The proposed energy producer mode is expected to achieve towards development of self sustainable dual-powered cellular networks, at much lower CAPEX.*

C. User QoS support and Operator revenue

In this subsection, we discuss the user QoS guarantee and revenue aspects of the proposed energy sharing framework. We compare the revenue results from the proposed framework with those presented in [20] and [22]. We have used the dual-powered WES framework considered in [20] as a baseline to show the gain in revenue through intelligent cooperative energy sharing among the BSs. It may be recalled that the CAPEX incurred with the strategy in [20] has been computed in Section V-A. Also, since the framework in [22] does not discuss the CAPEX provisioning and has not computed the optimal CAPEX required to design the dual-powered network, for a fair comparison, we have used the optimal CAPEX required in our framework to compare the optimal operator revenue in our approach as well as in [22]. The cost incurred to the operator in installation and maintenance of power lines (for a typical 69 kV overhead transmission line) has been taken from [41].

Fig. 7(a) represents the variation in user service revenue earned by the mobile network operator with increasing traffic inhomogeneity, through both the proposed energy producer and energy prosumer mode. It has been computed using the without coverage adjustment algorithm proposed in [13]. It may be noted that the user service revenue is similar for both the proposed modes of network operation and varies only with traffic skewness. Through Fig. 7(a) we also illustrate the variation of user service revenue with net user density in the considered area $\mathcal{A}$.

It can be observed that maximum user service revenue is earned when the network is subjected to homogeneous traffic and it decreases with increasing traffic inhomogeneity. User QoS guarantee in the network is measured in terms of the percent users unserved in the network. It can be observed from Fig. 7(a) that for both $\lambda_u = 2000$ and $\lambda_u = 3000$, the user QoS is satisfied only at $\zeta = 0$, i.e., when the traffic is homogeneous. We observe that user QoS decreases with increase in traffic skewness and touches about 24% at $\lambda = 2000$ and 30% at $\lambda_u = 3000$.

Remark 5. *The user QoS in the network decreases with increasing traffic inhomogeneity and results in decreasing the operator revenue earned from user service.*

Through Fig. 7(b), we illustrate the gain in sellable energy back to the power grid with varying levels of traffic inhomogeneity. It is observed that the proposed producer mode and prosumer mode perform similarly at lower levels of skewed traffic, with the proposed prosumer mode even bettering the producer mode at moderate skewed traffic (-1.07% gain at $\zeta = 0.3$). At higher skewness levels, the producer mode achieves significant gains over the producer mode, achieving up to 88% gain at extreme skewness levels.

It is notable that the WES framework presented in [20] does not deal with energy selling back to the grid. The gain in energy sold back to the grid through the proposed prosumer mode and producer mode of network operation over the framework presented in [22] is shown in Fig. 7(b). It can also be observed that while the proposed producer mode consistently attains a higher gain in energy selling, the gain in prosumer mode decreases sharply with the increase in traffic inhomogeneity. This is because, at lower traffic skewness the prosumer mode resorts to a higher energy selling to maximize profit. With an increase in traffic skewness, as the optimal CAPEX of the prosumer mode decreases, it resorts to an increased energy sharing, so as to maintain the operator revenue. The producer mode, on the other hand, consistently sells a higher fraction of energy as it is provisioned with a higher CAPEX.

The variation of net operator revenue and grid energy procurement for $\zeta = 1.2$ with increasing CAPEX is shown in Fig. 7(c). We see that while the optimum operator revenue is obtained at 0.6 $CAPEX^O$, the system becomes carbon free only at 0.8 $CAPEX^O$. Thus some additional CAPEX required must be provisioned with the BSs to make the system carbon free and self sustainable. The optimum revenue that the

Table IV: Revenue gain in the prosumer mode over the existing state of the art

ζ	0	0.3	0.7	1.2	1.5	2.5	3.0
Gain in prosumer over [20]	0.12%	32.26%	118.22%	100.72%	108.08%	42.03%	43.98%
Gain in prosumer over [22]	7.40%	8.92%	14.60%	5.28%	8.28%	7.38%	7.97%

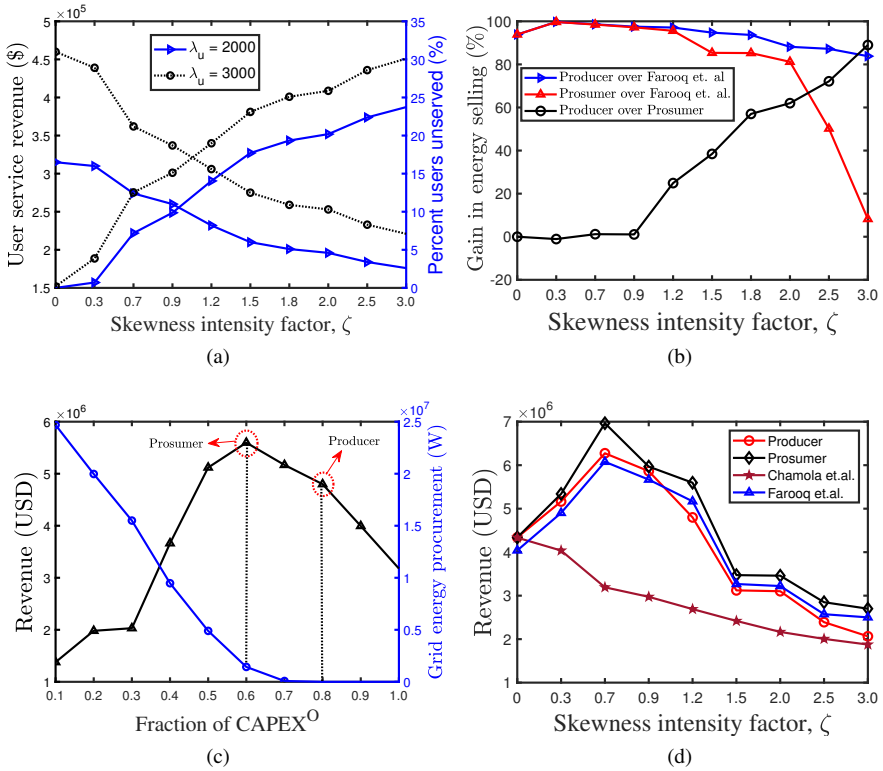

Figure 7: (a) User service revenue and QoS guarantee, (b) Gain in sellable energy, (c) Revenue and grid procurement variation at $\zeta = 1.2$, (d) Optimum operator revenue variation with ζ.

operator can earn in the dual-powered framework is termed the prosumer mode of network operation. On the other hand, the optimal CAPEX at which the system tends to be carbon free is called the energy producer mode of network operation.

Remark 6. *The energy producer mode incurs additional CAPEX in order to make the system carbon free as compared to the energy prosumer mode of network operation.*

Finally through Fig. 7(d), we illustrate the optimum revenue earned by the network operator through the proposed energy cooperative modes of network operation, the WES framework in [20], and an energy sharing framework in [22]. The operator revenue earned in the WES framework is observed to decrease with increasing traffic skewness. We observe that the energy prosumer mode significantly outperforms all the other frameworks, as shown in Table IV. It can be seen that the energy prosumer mode performs similar to the WES framework considered in [20] when subjected to homogeneous traffic. The prosumer mode obtains significantly higher gains with increasing traffic inhomogeneity and attains a gain up to 118.22% over [20] at $\zeta = 0.7$.

Similarly, it can be observed that the proposed energy prosumer mode consistently outperforms the energy sharing based framework in [22]. The prosumer mode is observed to attain a maximum gain of 14.6% at $\zeta = 0.7$. The framework in [22] is observed to perform poorly as compared to the proposed energy producer mode of operation up to $\zeta = 1.2$, but it outperforms the energy producer mode at higher skewness mainly due to the added CAPEX in the energy producer mode.

Remark 7. *The energy prosumer mode of network operation is able to efficiently exploit the traffic-energy imbalances in a dual-powered network, resulting in significant revenue gains with increase in traffic inhomogeneity.*

Remark 8. *The results demonstrate that in a dual-powered cellular scenario, moderate traffic inhomogeneity can lead to significant operator revenue gains compared to the homogeneous traffic case, but extreme traffic inhomogeneity results in degrading the system's performance.*

VI. Conclusion

An analytical framework has been presented in this paper to mathematically capture the traffic-energy imbalances in a dual-powered cellular network. The framework has demonstrated the benefits of exploiting these imbalances through a cooperative energy sharing based mechanism. The proposed networked energy sharing among the BSs has been facilitated via the power grid infrastructure itself. The significant ben-

efits of cooperative energy transfer have been demonstrated by designing the dual-powered communication system from two differentiating perspectives, namely, carbon emission or grid energy procurement minimization and operator revenue maximization. From the carbon emission perspective, a carbon free energy producer mode of operation has been proposed, wherein the BSs act as distributed energy source to the power grid. From the operator revenue perspective, an energy prosumer mode of operation has been proposed that involves an additional flexibility of grid energy procurement.

Both these perspectives have been independently formulated and optimized as convex problems. It has been observed that for a given CAPEX, the OPEX incurred in both these problems are identical. Optimal CAPEX and optimal revenue earned by the operator from both the perspectives have been computed using a linear optimization framework. The results demonstrate that cooperative energy transfer among the BSs is highly effective in reducing the CAPEX incurred to the operator as compared to the benchmark off-grid non-networked case. Further, the proposed energy prosumer mode has been observed to provide significant revenue gains over the other dual-powered frameworks. It is inferred that significant revenue gains can be achieved at moderate skewness in traffic, whereas extreme load skewness results in stretching the limits of traffic-energy balancing, thus degrading the system performance. It is expected that the proposed strategies will be highly beneficial to the mobile network operator and help in achieving green communication and lead towards the development of self-sustainable cellular networks.

APPENDIX

A. Derivation of BS downlink transmit power

Proof.

$$\mathcal{P}_b = \int_0^{R_b} \mathcal{P}_{ub}(y) f_Y(y) dy.$$
$$= \frac{\left[e^{(r_0 \ln 2\ \mathcal{U}_b/BW_b)} - 1\right]\left(BW_b\ \sigma^2\right) 2\pi\lambda_u}{\ln(1/p_0)\ \mathcal{U}_b} \int_0^{R_b} \left(y^3 e^{-\lambda_u \pi y^2}\right) dy \tag{A1}$$

$$\overset{(a)}{=} \frac{\left[e^{(r_0 \ln 2\ \mathcal{U}_b/BW_b)} - 1\right]\left(BW_b\ \sigma^2\right)}{\ln(1/p_0)\ \mathcal{U}_b} \left[-e^{-\lambda_u \pi t}\left(t + \frac{1}{\pi\lambda_u}\right)\right]_0^{R_b^2}$$
$$= \frac{\left[1 - e^{(r_0 \ln 2\ \mathcal{U}_b/BW_b)}\right]\left(BW_b\ \sigma^2\right) e^{-\lambda_u \pi R_b^2}}{\ln(p_0)\ \mathcal{U}_b}\left(R_b^2 + \frac{1}{\pi\lambda_u}\right) \tag{A2}$$

where, in step (a) we use the substitution $y^2 = t$. □

B. Proof of Lemma 1

Proof. To solve problem $\mathcal{P}2$, we define the Lagrangian of the primal problem $\mathcal{P}2$ as follows:

$$\mathbb{L}(\mathcal{S}_b, \lambda, \mu, \gamma) = \sum_{b=1}^{I} \left(\mathcal{S}_b(t)\right)^2 + \lambda\left(\sum_{b=1}^{I}\left(\mathcal{S}_b(t) - \mathcal{D}_b(t)\right)\right)$$
$$+ \mu\left(\sum_{b=1}^{I}\mathcal{S}_b(t) - \min\left\{\sum_{b'=1}^{J}\mathcal{E}_{b'}^S(t), \sum_{b=1}^{I}\mathcal{D}_b(t)\right\}\right) - \gamma\left(\sum_{b=1}^{I}\mathcal{S}_b(t)\right). \tag{B1}$$

Solving for $\partial\mathbb{L}(\mathcal{S}_b, \lambda, \mu, \gamma)/\partial\mathcal{S}_b = 0$, we get

$$\mathcal{S}_b^*(t) = \frac{(\gamma - \lambda - \mu)}{2}. \tag{B2}$$

$\mathcal{S}_b^*(t)$ represents the primal solution of problem $\mathcal{P}2$. To solve for the lagrange multipliers, we substitute the value of $\mathcal{S}_b^*(t)$ in $\mathbb{L}(\mathcal{S}_b, \lambda, \mu, \gamma)$, to obtain the dual function $g(\lambda, \mu, \gamma)$. The dual function obtained after substituting the primal solution in the lagrangian is given below.

$$g(\gamma, \lambda, \mu) = \frac{(\gamma - \lambda - \mu)^2 I}{4} + \frac{\lambda(\gamma - \lambda - \mu)I}{2} - \lambda\sum_{b=1}^{I}\mathcal{D}_b(t)$$
$$+ \frac{\mu(\gamma - \lambda - \mu)I}{2} - \mu\min\left\{\sum_{b'=1}^{J}\mathcal{E}_{b'}^S(t), \sum_{b=1}^{I}\mathcal{D}_b(t)\right\}$$
$$- \frac{\gamma(\gamma - \lambda - \mu)I}{2}$$
$$= \frac{-(\gamma - \lambda - \mu)^2 I}{4} - \lambda\sum_{b=1}^{I}\mathcal{D}_b(t)$$
$$- \mu\min\left\{\sum_{b'=1}^{J}\mathcal{E}_{b'}^S(t), \sum_{b=1}^{I}\mathcal{D}_b(t)\right\}. \tag{B3}$$

Solving the dual function for λ, i.e., $\partial g(\gamma, \lambda, \mu)/\partial\lambda = 0$, we get

$$(\gamma - \lambda - \mu)^* = \frac{2\sum_{b=1}^{I}\mathcal{D}_b(t)}{I}. \tag{B4}$$

Substituting the derived dual solution, $(\gamma - \lambda - \mu)^*$ in the primal solution (B2) gives

$$\mathcal{S}_b^*(t) = \sum_{b=1}^{I}\mathcal{D}_b(t)/I. \tag{B5}$$

Now, solving the dual function for γ, i.e., $\partial g(\gamma, \lambda, \mu)/\partial\gamma = 0$, we have

$$(\gamma - \lambda - \mu)^* = 0. \tag{B6}$$

On substituting (B6) in (B2), we get $\mathcal{S}_b^*(t) = 0$.

Finally, solving the dual function for μ, i.e., $\partial g(\gamma, \lambda, \mu)/\partial\mu = 0$, we get

$$(\gamma - \lambda - \mu) = \frac{2\min\left\{\sum_{b'=1}^{J}\mathcal{E}_{b'}^S(t), \sum_{b=1}^{I}\mathcal{D}_b(t)\right\}}{I} \tag{B7}$$

which on substituting in (B2) gives

$$\mathcal{S}_b^*(t) = \frac{\min\left\{\sum_{b'=1}^{J}\mathcal{E}_{b'}^S(t), \sum_{b=1}^{I}\mathcal{D}_b(t)\right\}}{I}. \tag{B8}$$

We observe that (B5) $\subset$ (B8). Hence (B8) is the optimum solution of the primal problem, $\mathcal{P}2$. (B8) can also be expressed as

$$\mathcal{S}_b^*(t) = \begin{cases} \sum_{b=1}^{I}\mathcal{D}_b(t)/I, & \text{if } \sum_{b=1}^{I}\mathcal{D}_b(t) \le \sum_{b'=1}^{J}\mathcal{E}_{b'}^S(t) \\ \sum_{b'=1}^{J}\mathcal{E}_{b'}^S(t)/I, & \text{if } \sum_{b=1}^{I}\mathcal{D}_b(t) > \sum_{b'=1}^{J}\mathcal{E}_{b'}^S(t) \end{cases} \tag{B9}$$

From (B9) we observe that $\mathcal{S}_b^*(t) = \sum_{b=1}^{I}\mathcal{D}_b(t)/I$ if $\sum_{b=1}^{I}\mathcal{D}_b(t) \le \sum_{b'=1}^{J}\mathcal{E}_{b'}^S(t)$. Intuitively, since we wish to reduce the grid-energy procurement, $\mathcal{S}_b^*(t) = \mathcal{D}_b(t)$ if $\sum_{b=1}^{I}\mathcal{D}_b(t) \le \sum_{b'=1}^{J}\mathcal{E}_{b'}^S(t)$. Thus, we see that

$\mathcal{S}_b(t) = \mathcal{D}_b(t) = \sum_{b=1}^{I} \mathcal{D}_b(t)/I$. Hence, for $\sum_{b=1}^{I} \mathcal{D}_b(t) > \sum_{b'=1}^{J} \mathcal{E}_{b'}^S(t)$, $\mathcal{S}_b(t)$ can be expressed as

$$\mathcal{S}_b(t) = \frac{\mathcal{D}_b(t) \sum_{b'=1}^{J} \mathcal{E}_{b'}^S(t)}{\sum_{b=1}^{I} \mathcal{D}_b(t)}. \tag{B10}$$

Thus, (B9) can be rewritten as

$$\mathcal{S}_b^*(t) = \begin{cases} \mathcal{D}_b(t), \text{ if } \sum_{b=1}^{I} \mathcal{D}_b(t) \leq \sum_{b'=1}^{J} \mathcal{E}_{b'}^S(t) \\ \mathcal{D}_b(t) \sum_{b'=1}^{J} \mathcal{E}_{b'}^S(t) / \sum_{b=1}^{I} \mathcal{D}_b(t), \\ \qquad \text{if } \sum_{b=1}^{I} \mathcal{D}_b(t) > \sum_{b'=1}^{J} \mathcal{E}_{b'}^S(t) \end{cases} \tag{B11}$$

or,

$$\mathcal{S}_b^*(t) = \frac{\mathcal{D}_b(t) \min\left\{\sum_{b'=1}^{J} \mathcal{E}_{b'}^S(t), \sum_{b=1}^{I} \mathcal{D}_b(t)\right\}}{\sum_{b=1}^{I} \mathcal{D}_b(t)}. \tag{B12}$$

The above equation (B12) represents the hourly optimal value of energy to be shared from energy-sufficient BSs to a deficient BS.

Since $\mathcal{G}_b(t) = \mathcal{D}_b(t) - \mathcal{S}_b(t)$, from (B12) we get

$$\mathcal{G}_b^*(t) = \begin{cases} 0, \text{ if } \sum_{b=1}^{I} \mathcal{D}_b(t) \leq \sum_{b'=1}^{J} \mathcal{E}_{b'}^S(t) \\ \mathcal{D}_b(t) \left(\frac{\sum_{b=1}^{I} \mathcal{D}_b(t) - \sum_{b'=1}^{J} \mathcal{E}_{b'}^S(t)}{\sum_{b=1}^{I} \mathcal{D}_b(t)}\right), \\ \qquad \text{if } \sum_{b'=1}^{J} \mathcal{E}_{b'}^S(t) < \sum_{b=1}^{I} \mathcal{D}_b(t). \end{cases} \tag{B13}$$

□

C. Proof of Theorem 1

Proof. The Lagrangian corresponding to the above primal problem is shown below.

$$\begin{aligned} \mathbb{L}\left(\mathcal{S}_b(t), \gamma, \mu\right) =& (C_b - C_{se} - C_{sh})^2 \sum_{b=1}^{I} \left(\mathcal{S}_b\right)^2 + \kappa - \gamma \sum_{b=1}^{I} \mathcal{S}_b \\ &+ \mu \left(\sum_{b=1}^{I} \mathcal{S}_b - \min\left\{ \sum_{b'=1}^{J} \mathcal{E}_{b'}^S, \sum_{b=1}^{I} \mathcal{D}_b \right\} \right). \end{aligned} \tag{C1}$$

Solving for $\partial \mathbb{L}\left(\mathcal{S}_b(t), \gamma, \mu\right) / \partial \mathcal{S}_b = 0$ yields

$$\mathcal{S}_b^* = \frac{(\gamma - \mu)}{2 \times (C_b - C_{se} - C_{sh})^2}. \tag{C2}$$

$\mathcal{S}_b^*$ represents the primal solution of $\mathcal{P}5$. We use the primal solution in (C2) to obtain the dual, which is given as

$$\begin{aligned} g(\gamma, \mu) =& \frac{I(\gamma - \mu)^2}{4(C_b - C_{se} - C_{sh})^2} + \kappa + \frac{(\mu\gamma - \mu^2)I}{2(C_b - C_{se} - C_{sh})^2} \\ &+ \frac{(\mu\gamma - \gamma^2)I}{2(C_b - C_{se} - C_{sh})^2} - \mu \min\left\{ \sum_{b'=1}^{J} \mathcal{E}_{b'}^S, \sum_{b=1}^{I} \mathcal{D}_b \right\}. \end{aligned} \tag{C3}$$

Solving for $\partial g(\gamma, \mu)/\partial \gamma = 0$, we get

$$\frac{-I(\gamma - \mu)}{2(C_b - C_{se} - C_{sh})^2} = 0. \tag{C4}$$

This results in $(\gamma - \mu) = 0$, or further $\mathcal{S}_b^* = 0$. Solving for $\partial g(\gamma, \mu)/\partial \mu = 0$, we get

$$\begin{aligned} &\frac{(\gamma - \mu)I}{2(C_b - C_{se} - C_{sh})^2} - \min\left\{ \sum_{b'=1}^{J} \mathcal{E}_{b'}^S, \sum_{b=1}^{I} \mathcal{D}_b \right\} = 0 \\ \text{or, } &(\gamma - \mu) = \frac{\min\left\{\sum_{b'=1}^{J} \mathcal{E}_{b'}^S, \sum_{b=1}^{I} \mathcal{D}_b\right\} \times 2(C_b - C_{se} - C_{sh})^2}{I} \end{aligned} \tag{C5}$$

The expression (C5) represents the dual solution of $\mathcal{P}5$. Substituting (C5) in the primal solution (C2), we get

$$\begin{aligned} \mathcal{S}_b^* &= \frac{\min\left\{\sum_{b'=1}^{J} \mathcal{E}_{b'}^S(t), \sum_{b=1}^{I} \mathcal{D}_b(t)\right\}}{I} \\ \text{or, } \mathcal{S}_b^*(t) &= \begin{cases} \mathcal{D}_b(t), \text{ if } \sum_{b=1}^{I} \mathcal{D}_b(t) \leq \sum_{b'=1}^{J} \mathcal{E}_{b'}^S(t) \\ \left(\mathcal{D}_b(t) \sum_{b'=1}^{J} \mathcal{E}_{b'}^S(t)\right) / \sum_{b=1}^{I} \mathcal{D}_b(t), \\ \qquad \text{if } \sum_{b'=1}^{J} \mathcal{E}_{b'}^S(t) < \sum_{b=1}^{I} \mathcal{D}_b(t). \end{cases} \end{aligned} \tag{C6}$$

From (25) and (C6), it can be observed that the optimal energy shared (and the corresponding grid energy procurement) to an energy-deficient BS in grid energy procurement minimization strategy is the same as that in operator revenue maximization strategy. Hence we prove that for a given CAPEX, the OPEX incurred in both optimization problems are identical. □

REFERENCES

[1] A. Balakrishnan, S. De, and L.-C. Wang, "Energy Sharing based Cooperative Dual-powered Green Cellular Networks," in *Proc. IEEE GLOBECOM, Madrid, Spain*, Dec. 2021, pp. 1–6.

[2] D. Wang, et al., "From IoT to 5G I-IoT: The Next Generation IoT-Based Intelligent Algorithms and 5G Technologies," *IEEE Communications Magazine*, vol. 56, no. 10, pp. 114–120, 2018.

[3] M. A. Marsan, et al., "Towards Zero Grid Electricity Networking: Powering BSs with Renewable Energy Sources," in *Proc. IEEE ICC Wksp., Budapest, Hungary*, June 2013.

[4] E. Oh, B. Krishnamachari, X. Liu, and Z. Niu, "Toward Dynamic Energy-efficient Operation of Cellular Network Infrastructure," *IEEE Commun. Mag.*, vol. 49, no. 6, pp. 56–61, 2011.

[5] "US Energy Information Administration (EIA), Carbon Dioxide Emission Coefficients." [Online]. Available: https://www.eia.gov/environment/

[6] J. G. Andrews, et al., "What Will 5G Be?" *IEEE J. Sel. Areas Commun.*, vol. 32, no. 6, pp. 1065–1082, 2014.

[7] Y. Chen, et al., "Fundamental Trade-offs on Green Wireless Networks," *IEEE Commun. Mag.*, vol. 49, no. 6, pp. 30–37, 2011.

[8] V. Chamola, et al., "Green Energy and Delay Aware Downlink Power Control and User Association for Off-Grid Solar-Powered Base Stations," *IEEE Syst. J.*, vol. 12, no. 3, pp. 2622–2633, 2018.

[9] F. Zhou, et al., "Computation Rate Maximization in UAV-Enabled Wireless-Powered Mobile-Edge Computing Systems," *IEEE J. Sel. Areas Commun.*, vol. 36, no. 9, pp. 1927–1941, 2018.

[10] F. Zhou, et al., "Artificial Noise Aided Secure Cognitive Beamforming for Cooperative MISO-NOMA using SWIPT," *IEEE J. Sel. Areas Commun.*, vol. 36, no. 4, pp. 918–931, 2018.

[11] M. Meo, et al., "Dimensioning the power supply of a LTE macro BS connected to a PV panel and the power grid," in *Proc. IEEE ICC*, 2015, pp. 178–184.

[12] D. Liu, et al., "Two-Dimensional Optimization on User Association and Green Energy Allocation for HetNets with Hybrid Energy Sources," *IEEE Trans. Commun.*, vol. 63, no. 11, pp. 4111–4124, 2015.

[13] A. Balakrishnan, S. De, and L.-C. Wang, "Network Operator Revenue Maximization in Dual Powered Green Cellular Networks," *IEEE Trans. Green Commun. Netw.*, vol. 5, no. 4, pp. 1791–1805, 2021.

[14] H. Jo, et al., "Heterogeneous Cellular Networks with Flexible Cell Association: A Comprehensive Downlink SINR Analysis," *IEEE Trans. Wireless Commun.*, vol. 11, no. 10, pp. 3484–3495, 2012.

[15] Z. Niu, et al., "Cell zooming for cost-efficient green cellular networks," *IEEE Commun. Mag.*, vol. 48, no. 11, pp. 74–79, 2010.

[16] E. Oh, K. Son, and B. Krishnamachari, "Dynamic Base Station Switching-On/Off Strategies for Green Cellular Networks," *IEEE Trans. Wireless Commun.*, vol. 12, no. 5, pp. 2126–2136, 2013.

[17] X. Liu and N. Ansari, "Profit-Driven User Association and Smart Grid Energy Transfer in Green Cellular Networks," *IEEE Trans. Veh. Tech.*, vol. 68, no. 10, pp. 10 111–10 120, 2019.

[18] H. Al Haj Hassan, et al., "A Novel Energy Model for Renewable Energy-Enabled Cellular Networks Providing Ancillary Services to the Smart Grid," *IEEE Trans. Green Commun. Netw.*, vol. 3, pp. 381–396, 2019.

[19] R. Ramamonjison and V. K. Bhargava, "Energy Allocation and Cooperation for Energy-Efficient Wireless Two-Tier Networks," *IEEE Trans. Wireless Commun.*, vol. 15, no. 9, pp. 6434–6448, 2016.

[20] V. Chamola, et al., "Delay Aware Resource Management for Grid Energy Savings in Green Cellular Base Stations with Hybrid Power Supplies," *IEEE Trans. Commun.*, vol. 65, no. 3, pp. 1092–1104, 2017.

[21] Y. Chia, S. Sun, and R. Zhang, "Energy Cooperation in Cellular Networks with Renewable Powered Base Stations," *IEEE Trans. Wireless Commun.*, vol. 13, no. 12, pp. 6996–7010, 2014.

[22] M. J. Farooq, et al., "A Hybrid Energy Sharing Framework for Green Cellular Networks," *IEEE Trans. Commun.*, vol. 65, no. 2, pp. 918–934, 2017.

[23] H.-S. Lee and J.-W. Lee, "Adaptive Traffic Management and Energy Cooperation in Renewable-Energy-Powered Cellular Networks," *IEEE Sys. J.*, vol. 14, no. 1, pp. 132–143, 2020.

[24] A. Paudel, et al., "Peer-to-Peer Energy Trading in Smart Grid Considering Power Losses and Network Fees," *IEEE Trans. Smart Grid*, vol. 11, no. 6, pp. 4727–4737, 2020.

[25] Y. Zhang, et al., "An overview of Energy-efficient Base Station Management Techniques," in *Proc. IEEE TIWDC*, 2013, pp. 1–6.

[26] A. Balakrishnan, S. De, and L.-C. Wang, "Traffic Skewness-aware Performance Analysis of Dual-powered Green Cellular Networks," in *Proc. IEEE GLOBECOM, Taipei, Taiwan*, Dec. 2020, pp. 1–6.

[27] Y. Zhong, T. Q. S. Quek, and X. Ge, "Heterogeneous Cellular Networks with Spatio-Temporal Traffic: Delay Analysis and Scheduling," *IEEE J. Sel. Areas Commun.*, vol. 35, no. 6, pp. 1373–1386, 2017.

[28] System Advisor Model: National Renewable Energy Laboratory. [Online]. Available: https://www.sam.nrel.gov

[29] G. Auer, et al., "How much energy is needed to run a Wireless Network?" *IEEE Wireless Commun.*, vol. 18, no. 5, pp. 40–49, 2011.

[30] N. Kwak and C.-H. Choi, "Input Feature Selection by Mutual Information based on Parzen Window," *IEEE Transactions on Pattern Analysis and Machine Intelligence*, vol. 24, no. 12, pp. 1667–1671, 2002.

[31] What will happen to solar panels after their useful lives are over? [Online]. Available: https://www.greenbiz.com

[32] S. Suman and S. De, "Low Complexity Dimensioning of Sustainable Solar-Enabled Systems: A Case of Base Station," *IEEE Trans. Sustain. Comput.*, vol. 5, no. 3, pp. 438–454, 2020.

[33] Antennae Location Methodology for a Telecomm Operator in India, IIM-B, Working paper no. 454. [Online]. Available: https://www.iimb.ac.in

[34] Economic Times-Solar Panel Cost: Price range of different types of solar panels and how much govt. subsidy you can avail for installing one. May 2014. [Online]. Available: https://economictimes.indiatimes.com

[35] 3GPP: A Global Initiative. [Online]. Available: https://www.3gpp.org/specifications

[36] Batteries for solar systems-Renewable Energy Batteries. [Online]. Available: https://www.thesolarbiz.com/batteries.html

[37] Technical Specification Group, Radio Access Network Meeting 99427. [Online]. Available: https://www.3gpp.org/ftp

[38] True Cost of Providing Energy to Telecomm Towers in India. [Online]. Available: https://www.gsma.com

[39] A. Goldsmith, *Wireless communications*. Cambridge university press, 2005.

[40] Economic Times-Falling solar power cost lead to pricing disputes. Nov. 2009. [Online]. Available: https://economictimes.indiatimes.com

[41] Power Grid International: Underground vs. Overhead, Power Line Installation-Cost Comparison and Mitigation. [Online]. Available: https://www.power-grid.com/

Ashutosh Balakrishnan (Graduate Student Member, IEEE) received the Bachelor of Technology (B. Tech.) degree with honors in electronics and telecommunication engineering from National Institute of Technology Raipur, India, in 2019. He is currently pursuing the Ph. D. degree from the Indian Institute of Technology Delhi, New Delhi, India, under IIT Delhi – NYCU Taiwan Joint Doctoral Program. He is a current recipient of the prestigious Prime Minister's Research Fellowship, Govt. of India. His research interests include wireless communication networks, energy harvesting, machine learning, optimization, green communication, and cross-layer design.

Swades De (Senior Member, IEEE) received the B.Tech. degree in Radiophysics and Electronics from the University of Calcutta in 1993, the M.Tech. degree in Optoelectronics and Optical Communication from IIT Delhi in 1998, and the Ph.D. degree in Electrical Engineering from the State University of New York at Buffalo in 2004.

Dr. De is currently a Professor with the Department of Electrical Engineering, IIT Delhi. Before moving to IIT Delhi in 2007, he was a Tenure-Track Assistant Professor with the Department of ECE, New Jersey Institute of Technology, Newark, NJ, USA, from 2004–2007. He worked as an ERCIM Post-doctoral Researcher at ISTI-CNR, Pisa, Italy (2004), and has nearly five years of industry experience in India on telecom hardware and software development, from 1993–1997, 1999. His research interests are broadly in communication networks, with emphasis on performance modeling and analysis. Current directions include energy harvesting wireless networks, broadband wireless access and routing, network coexistence, smart grid networks, and IoT communications. Dr. De currently serves as an Area Editor of IEEE COMMUNICATIONS LETTERS and Elsevier Computer Communications, and an Associate Editor of IEEE TRANSACTIONS ON VEHICULAR TECHNOLOGY and IEEE WIRELESS COMMUNICATIONS LETTERS.

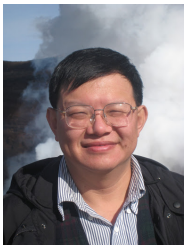

Li-Chun Wang (Fellow, IEEE) received Ph. D. degree from the Georgia Institute of Technology, Atlanta, in 1996. From 1996 to 2000, he worked at AT&T Laboratories, where he was a Senior Technical Staff Member in the Wireless Communications Research Department. Since August 2000, he has joined the Department of Electrical and Computer Engineering at National Yang Ming Chiao Tung University in Taiwan. He is now a Chair Professor and is jointly appointed by the Department of Computer Science and Information Engineering from the same university.

Dr. Wang was elected to an IEEE Fellow in 2011 for his contributions to cellular architecture and radio resource management in wireless networks. He has won two Distinguished Research Awards from Taiwan's Ministry of Science and Technology (2012, 2017). He was the co-recipients of IEEE Communications Society Asia-Pacific Board Best Award (2015), Y. Z. Hsu Scientific Paper Award (2013), and IEEE Jack Neubauer Best Paper Award (1997).

His recent research interests are in the areas of cross-layer optimization for wireless systems, data-driven radio resource management, software-defined heterogeneous mobile networks, big data analysis for industrial Internet of things, and AI-enabled unmanned aerial vehicular (UAV) networks. He holds 26 US patents, and has published over 300 journal and conference papers, and co-edited the book, "Key Technologies for 5G Wireless Systems," (Cambridge University Press 2017).